Interaction and structuration of membrane-binding and membrane-excluding colloidal particles in lamellar phases

Ruben Zakine, Dasith de Silva Edirimuni, Doru Constantin, Paolo Galatola, Jean-Baptiste Fournier

HAL Id: hal-02349525
https://hal.science/hal-02349525

Submitted on 5 Nov 2019

Interaction and self-assembly of membrane-binding
and membrane-excluding colloids embedded in lamellar phases

Ruben Zakine[a], Dasith de Silva Edirimuni[a], Doru Constantin[b], Paolo Galatola[a] and Jean-Baptiste Fournier[*a]

[a]Laboratoire"Matière et Systèmes Complexes" (MSC), UMR 7057 CNRS,
Université Paris 7 Diderot, 75205 Paris Cedex 13, France.
[b]Laboratoire de Physique des Solides, CNRS, Université Paris-Sud, Université Paris-Saclay, 91405 Orsay Cedex, France.

Within the framework of a discrete Gaussian model, we present analytical results for the interaction induced by a lamellar phase between small embedded colloids. We consider the two limits of particles strongly adherent to the adjacent membranes and of particles impenetrable to the membranes. Our approach takes into account the finite size of the colloids, the discrete nature of the layers, and includes the Casimir-like effect of fluctuations, which is very important for dilute phases. Monte Carlo simulations of the statistical behavior of the membrane-interacting colloids account semi-quantitatively, without any adjustable parameters, for the experimental data measured on silica nanospheres inserted within lyotropic smectics. We predict the existence of finite-size and densely packed particle aggregates originating from the competition between attractive interactions between colloids in the same layer and repulsion between colloids one layer apart.

I. INTRODUCTION

Assembling nanoparticles into organized superstructures is one of the most important topics in contemporary materials science. The sought-for organization concerns positional order, since the properties of the individual particles can be tuned via coupling to their neighbors, yielding enhanced or even completely novel characteristics (as for metamaterials). However, the orientational order is equally important: in the case of anisotropic nanoparticles, aligning them is an essential step towards propagating this anisotropy to the macroscopic scale of the final material. Other important requirements concern the finite size of the resulting assemblies and their shape (e.g. elongated, flat, isometric etc.).

In this context, using liquid crystal matrices, which are both ordered and soft (and thus easily processable) is a promising design option for hybrid materials with original properties [1]. Many groups have employed this strategy, using either nematic phases (which only exhibit orientational order) [2, 3] or smectic phases (with an additional positional order) [4–6]. It is clear that the fundamental problem of the interaction between inclusions in liquid crystals can have very practical applications.

The examples above concern thermotropic phases (consisting of a single type of molecules). Another large class of systems is that of lyotropic phases, where self-assembled entities (micelles, bilayers, etc.) are dispersed in a (usually aqueous) solvent.

Lyotropic liquid crystals are particularly suitable for controlling the self-assembly process, because their elastic moduli are lower than those of thermotropics, so that the induced interactions can be weaker (comparable to $k_B T$) and because their properties (spacing, flexibility, electrical charge etc.) are easily tuned via the composition [7, 8]. In addition, their intrinsically heterogeneous nature (bilayers of amphiphilic molecules separated by water layers) opens the possibility of confining within the same phase particles with different chemical affinities [9, 10].

For all these reasons, particle inclusions in lyotropic phases have raised the interest of numerous groups all over the world [11]. Both the structuring effect of the host lamellar phase on the inclusions [12] and the influence of the latter on the dispersing phase [13] have been studied.

The distinctive features of lyotropic phases must also be accounted for in a realistic model for the induced interactions: i) The boundary conditions must be stated in terms of particle interaction with discrete (and generally impenetrable) bilayers rather than with a continuous director field. ii) These soft systems exhibit strong fluctuations, so the model should take into account fluctuation-induced, Casimir-like interactions.

The model presented here deals with lamellar lyotropic phases and includes both these aspects. Using a discrete Gaussian description [14–16], we treat the coupling between the lamellae and the colloids in an almost exact manner. The fluctuations are accounted for rigorously, since the interaction results from an integral over all membrane configurations. In terms of boundary conditions, we consider two types of colloids: membrane-binding, which adhere strongly to the neighboring bilayers, and membrane-excluding, which exhibit hard-core repulsion with respect to the membranes. The adhesion and the repulsion are considered very strong with respect to the other energy scales in the problem, so the colloid is simply described by its diameter. In both cases the membrane-colloid coupling is nonlinear. Interestingly, for membrane-excluding colloids smaller than the membrane separation, the situation is analogous to the Casimir effect, since the presence of the colloids merely suppresses fluctuation modes of the lamellar phase.

Our paper is organized as follows. In Section II, we describe our model of the lamellar phase [14–16] and we describe the lamellae fluctuations. In Section III A, we study the interactions between membrane-binding colloids and the deformations they create in the membrane. In Section III B, we study the interactions between membrane-excluding colloids and the deformations they create in the membrane. In Section IV we investigate the equilibrium statistical behavior of the interacting colloids and their self-assembly by Monte Carlo simulations. In Section V, we compare our simulations to the experimental results of ref. 17. Finally, in Section VI

we resume our results and we conclude.

II. LAMELLAR PHASE MODEL

Lamellar phases are stacks of membranes in an aqueous environment. Membranes interact through different mechanisms: attractive van der Waals forces, repulsive hydration forces at very short separations, screened electrostatic forces, and the so-called Helfrich long-range repulsion arising from the loss of entropy associated with the confinement of the transverse membrane fluctuations [18]. The latter may dominate for membranes with weak bending rigidities, i.e., typically for surfactant systems [19]. There may also be attractive fluctuation–induced interactions originating from counterion correlations [20].

Lipids form lamellar phases of bilayer membranes where the layer spacing d is usually comparable to the membrane thickness δ, i.e., a few nm. Conversely, surfactant systems can form lamellar phases with $d \gg \delta$, and even unbound lamellar phases. An exact theoretical modelization of the elasticity of lamellar phases, taking into account all the different interactions, is very difficult to achieve. We therefore limit ourselves to the discrete Gaussian elastic theory of lamellar phase [14–16], as described below.

We consider a lamellar phase consisting of N parallel membranes of thickness δ (see Fig. 1). We assume that in the homogeneous, equilibrium state, the thickness of the water layers between the membranes is w and the repeat distance is d, with

$$d = w + \delta. \tag{1}$$

In a Cartesian reference frame $(\boldsymbol{r}, z) \equiv (x, y, z)$, we parametrize the shape of the n-th membrane by the height function $z_n(\boldsymbol{r}) = nd + h_n(\boldsymbol{r})$, which represents its elevation above the plane $z = 0$. In addition to the bending energy of each membrane [21], the elastic energy includes the most general interaction that is quadratic in the h_n's, couples only adjacent membranes, and complies with global translational invariance [14–16]:

$$\mathcal{H} = \sum_{n=0}^{N-1} \int d^2r \left[\frac{\kappa}{2} \left(\nabla^2 h_n \right)^2 + \frac{B}{2} \left(h_{n+1} - h_n \right)^2 \right]. \tag{2}$$

Here, κ is the bending stiffness of the membranes and B is an effective compression modulus, which accounts for all the interactions between the layers. Note that we have assumed that the membrane undulations are gentle enough so that the Gaussian approximation of the curvature energy can be used [21]. The bulk moduli for layer compression and layer curvature [22] are $B_3 = Bd$ and $K = \kappa/d$, respectively.

It is convenient to work with dimensionless quantities. We use $k_{\mathrm{B}}T$ to normalize the energies, $\xi = (\kappa/B)^{1/4}$ to normalize the lengths parallel to (x, y), and $\xi_{\parallel} = \xi\sqrt{k_{\mathrm{B}}T/\kappa}$ to normalize h_n and all the lengths parallel to z, including d, δ, w and the colloid diameters, hereafter called a and b. The characteristic lengths ξ and $\xi_{\parallel}$ are linked to the de Gennes
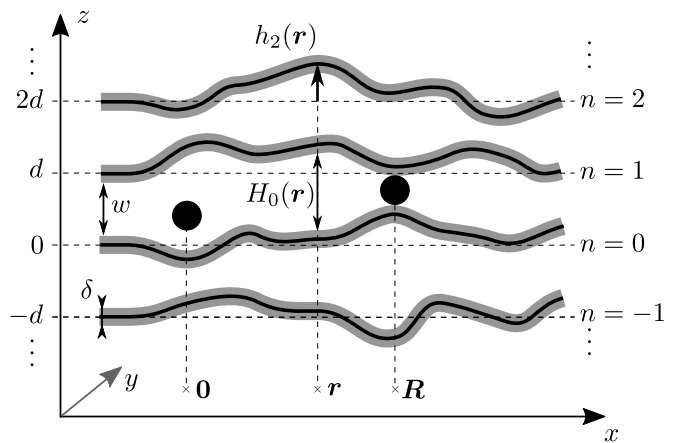

FIG. 1. Parametrization of the lamellar phase (cross section). The membranes, of thickness δ, are drawn in gray and their midsurfaces are represented as black lines. The average lamellar spacing and water thickness are d and w, respectively. The layer displacements are described by the functions $h_n(\boldsymbol{r})$ and the gap between the layers by the functions $H_n(\boldsymbol{r})$, as indicated. Two colloids are represented as black disks: the one on the left is a membrane-excluding colloid having only excluded volume interactions with the membranes, the one on the right is a membrane-binding colloid that sticks to the membranes.

penetration length λ [22] and to the Caillé exponent η [23] by the relations $\xi = \sqrt{\lambda d}$ and $\xi_{\parallel} = d\sqrt{2\eta/\pi}$. From now on, unless otherwise specified, all quantities will be in dimensionless form. Thus, the Hamiltonian (2) becomes

$$\mathcal{H} = \sum_{n=0}^{N-1} \int d^2r \left[\frac{1}{2} \left(\nabla^2 h_n \right)^2 + \frac{1}{2} \left(h_{n+1} - h_n \right)^2 \right]. \tag{3}$$

It is also convenient to work in Fourier space. We thus define

$$h_n(\boldsymbol{r}) = \frac{1}{L\sqrt{N}} \sum_{Q,\boldsymbol{q}} h_{Q,\boldsymbol{q}} e^{iQnd} e^{i\boldsymbol{q}\cdot\boldsymbol{r}}, \tag{4}$$

with L the lateral size of the membrane. Assuming periodic boundary conditions in all directions, the wavevectors are quantified according to $Q = 2\pi m/(Nd) \in [-\pi/d, \pi/d[$ and $\boldsymbol{q} = (q_x, q_y) = (2\pi m/L, 2\pi\ell/L)$, with $m, \ell \in \mathbb{Z}$. The elastic Hamiltonian takes then the simple form [16]:

$$\mathcal{H} = \sum_{Q,\boldsymbol{q}} \frac{1}{2} A(Q, q) h_{Q,\boldsymbol{q}} h_{-Q,-\boldsymbol{q}}, \tag{5}$$

with

$$A(Q, q) = q^4 + 2(1 - \cos Qd). \tag{6}$$

A. Orders of magnitude

Typical values for the elastic parameters of lipid and surfactant lamellar phases are given below and listed in Table I.

TABLE I. Elastic parameters for typical lipid and surfactant membranes. The last three lengths are in dimensionless units.

	κ (J)	B (J m^{-4})	ξ; $\xi_\parallel$ (nm)	δ	w	d
Egg PC	0.5×10^{-19}	1×10^{15}	2.7; 0.75	5.3	1.3	6.6
$C_{12}E_5$	3.7×10^{-21}	6×10^8	50; 52	0.06	0.74	0.79

1. Lipid membranes

For lamellar phases made of egg PC lipids [24], the elastic constants are $\kappa \simeq 0.5 \times 10^{-19}$ J, and typically $B \simeq 1 \times 10^{15}$ J m^{-4} for $w \simeq 1$ nm, with $\delta \simeq 4$ nm and $d \simeq 5$ nm. We thus obtain $\xi = (\kappa/B)^{1/4} \simeq 2.7$ nm and $\xi_\parallel = \sqrt{k_B T}/(B\kappa)^{1/4} \simeq 0.75$ nm, yielding in dimensionless form $\delta \simeq 5.3$, $w \simeq 1.3$ and $d \simeq 6.6$.

2. Surfactant membranes

For the $C_{12}E_5$/hexanol/water system [17, 25], with typically a hexanol/$C_{12}E_5$ ratio of 0.35 and a membrane fraction of $\phi \simeq 7\%$, the elastic constants are $\kappa \simeq 3.7 \times 10^{-21}$ J and $B \simeq 6 \times 10^8$ J m^{-4}, with $\delta \simeq 2.9$ nm, $d = \delta/\phi \simeq 41.5$ nm and $w \simeq 38.5$ nm. We thus obtain $\xi = (\kappa/B)^{1/4} \simeq 50$ nm, $\xi_\parallel = \sqrt{k_B T}/(B\kappa)^{1/4} \simeq 52$ nm, yielding in dimensionless form $\delta \simeq 0.055$, $w \simeq 0.74$ and $d \simeq 0.79$.

B. Fluctuations

The fluctuations of the lamellar phase (in the absence of colloids) are obtained in a standard way by adding an external field $J_{Q,q}$ to the partition function [26]:

$$Z[J] = \int \left(\prod_{n=0}^{N-1} \mathcal{D}[h_n] \right) \exp\left(-\mathcal{H} + \sum_{Q,q} J_{-Q,-q} h_{Q,q} \right)$$

$$= Z_0 \exp\left(\sum_{Q,q} \frac{J_{Q,q} J_{-Q,-q}}{A(Q,q)} \right), \tag{7}$$

where Z_0 is the partition function of the lamellar phase. We shall denote by $\langle \ldots \rangle$ the statistical average over the membrane fluctuations. By differentiation, we obtain

$$\langle h_{Q,q} h_{Q',q'} \rangle = \left. \frac{\partial^2 \ln Z}{\partial J_{-Q,-q} \partial J_{-Q',-q'}} \right|_{J=0} = \frac{\delta_{Q+Q'} \delta_{q+q'}}{A(Q,q)}. \tag{8}$$

The *gap* between layers p and $p+1$, at position r, is given by

$$H_p(r) = w + h_{p+1}(r) - h_p(r). \tag{9}$$

Its average $\langle H_p(r) \rangle$ is w. Using eqns (4) and (8), we obtain its correlation function

$$\langle H_0(\mathbf{0}) H_p(r) \rangle - w^2 = \frac{2}{NL^2} \sum_{Q,q} \frac{1 - \cos Qd}{A(Q,q)} e^{iQpd} e^{iq \cdot r}$$

$$= \frac{G_p(r)}{2\pi}, \tag{10}$$

where the factor 2π was introduced for later convenience. In the thermodynamic limit,

$$G_p(r) = \frac{1}{\pi} \int_{-\pi}^{\pi} d\phi \int_0^\infty dq \frac{q(1 - \cos\phi)\cos(p\phi) J_0(qr)}{q^4 + 2(1 - \cos\phi)}, \tag{11}$$

with, in particular, $G_0(0) = 1$, $G_0(r) = 2 J_1(r) K_1(r)$, where J_1 and K_1 are Bessel functions (see the Appendix), $G_p(0) = 1/(1 - 4p^2)$ and $G_p(\infty) = 0$.

It follows that the standard deviation of the gap, or, equivalently of the layer spacing, is given by $\sigma = \sqrt{G_0(0)/(2\pi)} = 1/\sqrt{2\pi}$. In dimensionful form, this gives $\sigma = \xi \sqrt{k_B T/(2\pi\kappa)}$ (in agreement with ref. 24). Note that our Gaussian Hamiltonian (2) takes into account the repulsion of the layers by means of a soft harmonic repulsive potential. Since the layers cannot physically interpenetrate, the consistency of the model requires $w \gtrsim \sigma$, i.e., in dimensionless form, $w \gtrsim 1/\sqrt{2\pi} \simeq 0.4$. Note that this condition is true for the parameters given above (see Table I).

Let us also compute the correlation between the membrane gaps and the layer displacements, that will show up in the calculation of the deformation of the lamellar phase induced by the colloids:

$$\Gamma_p(r) = 2\pi \langle H_0(\mathbf{0}) h_p(r) \rangle = \frac{2\pi}{NL^2} \sum_{Q,q} \frac{e^{-iQd} - 1}{A(Q,q)} e^{iQpd} e^{iq \cdot r}. \tag{12}$$

In the thermodynamic limit,

$$\Gamma_p(r) = \frac{1}{2\pi} \int_{-\pi}^{\pi} d\phi \int_0^\infty dq \frac{q(e^{-i\phi} - 1) e^{ip\phi} J_0(qr)}{q^4 + 2(1 - \cos\phi)}, \tag{13}$$

with, in particular, $\Gamma_p(0) = 1/(4p - 2)$ and $\Gamma_p(\infty) = 0$.

III. INTERACTIONS BETWEEN COLLOIDAL PARTICLES

Sens and Turner studied the interactions between particles in lamellar phases in a series of papers [27–30]. They described the particles by pointlike couplings inducing either a local pinching, a local stiffening or a local curvature of the membrane. Dealing with both thermotropic and lyotropic smectics, they used the three-dimensional smectic elasticity expressed in terms of a continuous layer displacement function [31]. This approach yields the asymptotic interaction between colloids and thus the collective phase behavior when the colloids are dispersed, but the obtained interaction has a peculiar divergence for colloids in the same layer.

An approximate cure to this problem was proposed in ref. 32 by the introduction of a high wavevector cutoff of the order of the inverse smectic spacing. Another difficulty, inherent to linear couplings, is that the fluctuation corrections to the interactions are not accounted for. For smectics, since colloids are always significantly larger than the smectic period, modeling a colloid in a more realistic manner requires introducing a multipolar development [29], or an effective coat larger than the particle where the deformation is small enough to use a multipolar approach [32]. Choosing the multipoles coefficients is difficult, however, in particular because enforcing strict boundary conditions make them in general dependent on the distances between the colloids. Finally, as shown in ref. 33, rotational invariance and the associated non-linear effects can yield important modifications in the far-field deformations and thus in the interaction potentials.

In this study, as discussed in Section I, we use a different approach, based on a discrete model for the layers. This approach applies to lyotropic lamellar phases, but not to continuous smectic phases. It has the advantage, however, that the colloid-lamellar coupling is taken into account in an almost exact manner. We therefore expect to obtain reliable interactions at all separations, including in particular the fluctuation-induced corrections.

A. Membrane-binding colloids

Let us start by considering colloids that adhere strongly to the neighboring bilayers, as the colloid on the right in Fig. 1. We consider a first colloid of diameter a binding to layers $n = 0$ and $n = 1$ at the in-plane position $(x, y) = \mathbf{0}$, and a second one of diameter b binding to layers $n = p$ and $n = p + 1$ at the in-plane position $(x, y) = \mathbf{R}$. We model their binding as a simple constraint on the gaps between their neighboring membranes on the axis normal to the undeformed membranes:

$$H_0(\mathbf{0}) = a, \quad H_p(\mathbf{R}) = b. \tag{14}$$

The partition function of the system (at fixed projected positions, $\mathbf{0}$ and $\mathbf{R}$, of the colloids) is therefore given by

$$Z_{\text{bind}} = \int \left(\prod_{n=0}^{N-1} \mathcal{D}[h_n] \right) \delta(H_0(\mathbf{0}) - a)\, \delta(H_p(\mathbf{R}) - b)\, e^{-\mathcal{H}}. \tag{15}$$

Using the Fourier representation both of the delta functions and of the layer displacements yields:

$$Z_{\text{bind}} = \int \left(\prod_{n=0}^{N-1} \mathcal{D}[h_n] \right) \frac{d\lambda}{2\pi} \frac{d\mu}{2\pi}\, e^{i\lambda(w-a)+i\mu(w-b)}$$
$$\times e^{-\sum_{Q,\boldsymbol{q}} \left[\frac{1}{2} A(Q,q) h_{Q,\boldsymbol{q}} h_{-Q,-\boldsymbol{q}} - h_{Q,\boldsymbol{q}} S_{-Q,-\boldsymbol{q}} \right]}, \tag{16}$$

with

$$S_{Q,\boldsymbol{q}} = i\lambda \frac{e^{-iQd}-1}{L\sqrt{N}} + i\mu \frac{e^{-iQd}-1}{L\sqrt{N}} e^{-iQpd} e^{-i\boldsymbol{q}\cdot\boldsymbol{R}} + J_{Q,\boldsymbol{q}}, \tag{17}$$

where we have added an external field $J_{Q,\boldsymbol{q}}$ that will be used to compute the average deformation of the lamellar phase in the presence of the colloids. Performing the Gaussian integrals, and discarding irrelevant constant factors, yields

$$Z_{\text{bind}} = \int d\lambda\, d\mu\, e^{i\lambda(w-a)+i\mu(w-b)} e^{\frac{1}{2}\sum_{Q,\boldsymbol{q}} \frac{1}{A(Q,q)} S_{Q,\boldsymbol{q}} S_{-Q,-\boldsymbol{q}}}$$
$$= (\det M)^{-1/2} e^{-\frac{1}{2}(s,s') M^{-1}(s,s')^T}$$
$$\times e^{\frac{1}{2}\sum_{Q,\boldsymbol{q}} \frac{1}{A(Q,q)} J_{Q,\boldsymbol{q}} J_{-Q,-\boldsymbol{q}}}, \tag{18}$$

where $M(R, p)$ is a symmetric 2×2 matrix with elements:

$$M_{11} = M_{22} = \frac{2}{NL^2} \sum_{Q,\boldsymbol{q}} \frac{1-\cos Qd}{A(Q,q)} = \frac{G_0(0)}{2\pi},$$

$$M_{12} = \frac{2}{NL^2} \sum_{Q,\boldsymbol{q}} \frac{1-\cos Qd}{A(Q,q)} \cos(Qpd + \boldsymbol{q}\cdot\boldsymbol{R}) = \frac{G_p(R)}{2\pi}, \tag{19}$$

where we recognize the correlation function of the layer spacing, and

$$s = w - a + \frac{1}{L\sqrt{N}} \sum_{Q,\boldsymbol{q}} J_{Q,\boldsymbol{q}} \frac{e^{iQd}-1}{A(Q,q)}, \tag{20}$$

$$s' = w - b + \frac{1}{L\sqrt{N}} \sum_{Q,\boldsymbol{q}} J_{Q,\boldsymbol{q}} \frac{e^{iQd}-1}{A(Q,q)} e^{iQpd} e^{i\boldsymbol{q}\cdot\boldsymbol{R}}. \tag{21}$$

1. Interaction free energy and average deformation

Taking the thermodynamic limit $N \to \infty$ and $L \to \infty$, we obtain for $J_{Q,\boldsymbol{q}} = 0$, apart from an irrelevant constant factor,

$$Z_{\text{bind}} = \left(1 - G_p(R)^2\right)^{-1/2}$$
$$\times e^{-\pi \frac{(a-w)^2 + (b-w)^2 - 2G_p(R)(a-w)(b-w)}{1 - G_p(R)^2}} \tag{22}$$

The total free energy $-\ln(Z_{\text{bind}})$ of the system yields, after subtracting the value for infinitely separated colloids, the interaction free energy of the two colloids:

$$F_{\text{bind}}(R, p) = F_{\text{bind}}^{\text{Cas}}(R, p) + F_{\text{bind}}^{\text{el}}(R, p) \tag{23}$$

$$F_{\text{bind}}^{\text{Cas}} = \frac{1}{2} \ln \left(1 - G_p(R)^2\right), \tag{24}$$

$$F_{\text{bind}}^{\text{el}} = -\frac{2\pi G_p(R)}{1 + G_p(R)} \left[(a-w)(b-w) - \frac{1}{2} \frac{G_p(R)(a-b)^2}{1 - G_p(R)} \right]. \tag{25}$$

In order to get the dimensionful form of these interactions, one has to multiply these expressions by $k_{\text{B}}T$ and add an extra factor $\sqrt{\kappa B}/k_{\text{B}}T$ in front of $(w-a)(w-b)$ and $(a-b)^2$. The interaction $F_{\text{bind}}^{\text{Cas}}$, which is thus directly proportional to the temperature, is a Casimir-like interaction, caused by the
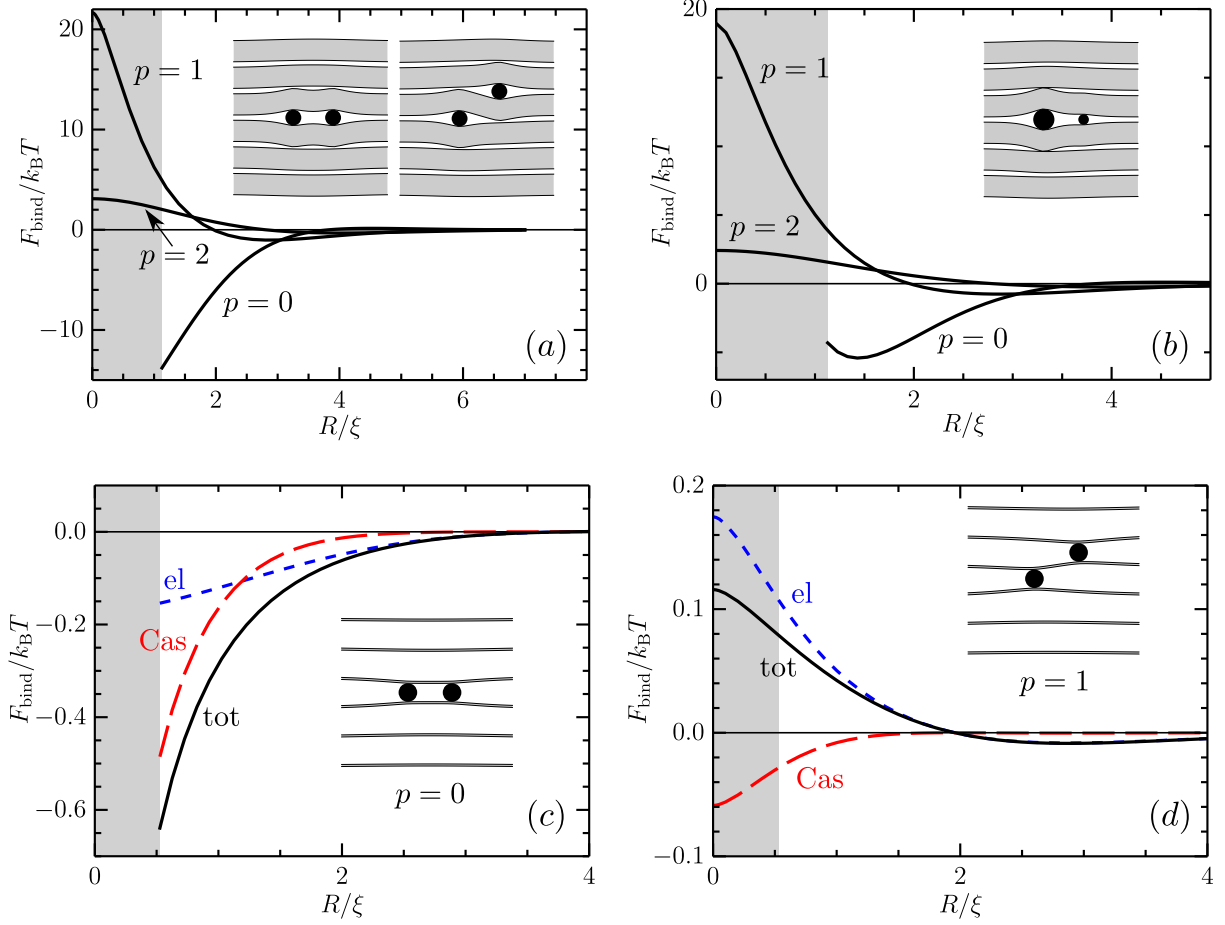
FIG. 2. (a) Interaction energy as a function of separation for membrane-binding colloids with diameters $a = b = 3w$ in a lamellar phase with the parameters of egg PC (see Section II A 1). The Casimir contribution to the interaction is less than 1% of the elastic part. Colloids in the same layer ($p = 0$), one layer apart ($p = 1$), two layers apart ($p = 2$). Insets: Deformations of the lamellar phase, calculated numerically using eqn (27), for $R/d = 1.5$ and $N = 100$. The membranes, in gray, and the colloids, in black, are represented at scale. (b) Same as (a) for colloids of diameter $a = 4w$ and $b = 2w$. (c) Interaction energy as a function of separation for binding colloids of diameter $a = b = 0.7w$ placed in the same layer in a lamellar phase with the parameters of $C_{12}E_5$ (see Section II A 2). Black solid line (tot): total interaction F_{bind}. Blue dashed line (el): elastic interaction $F_{\text{bind}}^{\text{el}}$. Red long-dashed line (Cas): Casimir interaction $F_{\text{bind}}^{\text{Cas}}$. Inset: numerically calculated deformation of the lamellar phase, using eqn (27), for $R/d = 1.5$ and $N = 100$. The membranes and the colloids are represented at scale. (d) Same but for colloids one layer apart ($p = 1$).

restriction of the fluctuations induced by the binding of the colloids. The interaction $F_{\text{bind}}^{\text{el}}$ is an athermal "elastic" interaction, proportional to $\sqrt{\kappa B}$ (it depends on temperature only through κ and B) and it is caused by the deformation of the layers induced by the colloids. Note that if $a = b = w$, in which case the colloids do not deform the layers, the elastic interaction vanishes while the fluctuation-induced Casimir interaction remains.

The average deformation of the lamellar phase is given by

$$\langle h_{-Q,-\boldsymbol{q}} \rangle_{\text{bind}} = \left. \frac{\partial \ln Z_{\text{bind}}}{\partial J_{Q,\boldsymbol{q}}} \right|_{J=0}$$
$$= -\frac{1}{2} \left. \frac{\partial \left[(s,s') M^{-1}(s,s')^T \right]}{\partial J_{Q,\boldsymbol{q}}} \right|_{J=0}, \quad (26)$$

yielding

$$\langle h_n(\boldsymbol{r}) \rangle_{\text{bind}} = \frac{a - w - G_p(R)(b-w)}{1 - G_p(R)^2} \Gamma_n(r)$$
$$+ \frac{b - w - (a-w)G_p(R)}{1 - G_p(R)^2} \Gamma_{n-p}(|\boldsymbol{r} - \boldsymbol{R}|), \quad (27)$$

where Γ_n is the correlation function (12). The deformation induced by just one colloid, of diameter a, is obtained by taking the first term in the right-hand side of eqn (27) for $G_p(R) = 0$ (infinite separation) and is given by

$$\langle h_n^{(1)}(\boldsymbol{r}) \rangle_{\text{bind}} = (a - w)\Gamma_n(r). \quad (28)$$

Note that the deformation set by two colloids is not simply the superposition of the deformations set by each individual col-

loid. This non-linearity comes from the membrane thickness constraint imposed by the particles.

The deformation above a single colloid, of diameter a, placed between layers 0 and 1, is therefore given by

$$\langle h_n^{(1)}(\mathbf{0})\rangle_{\text{bind}} = \frac{a - w}{4n - 2} \, . \tag{29}$$

It is independent of the elastic constants since a, w, and h_n are normalized with respect to the same length.

For the consistency of our model, we must verify that the gap between the membranes bound to the colloids and the adjacent ones remain positive despite the deformation. In particular, we must have $\langle H_1(\mathbf{0})\rangle > 0$. Given eqns (29) and (9), this yields the consistency condition $0 < a < 4w$ for a colloid of diameter a.

2. Typical results

Lamellar phases made with lipids have a layer spacing typically comparable, or even smaller, than the membrane thickness $\simeq 4\,\text{nm}$, so that only nano-colloids will fit in such systems (see Section II A 1). We show in Fig. 2a the typical interaction energy between membrane-binding colloids and the corresponding lamellar phase deformation. The values correspond to egg PC lipids with colloids of diameters $\simeq 3\,\text{nm}$. Two colloids in the same layer attract each other, while colloids in different layers repel one another. The maximum interaction energies are large with respect to $k_{\text{B}}T$. When the colloids are separated by more than one empty layer, their interaction becomes negligible compared to $k_{\text{B}}T$. For such lipid lamellar phases the Casimir component of the interaction energy is always negligible with respect to the elastic one. In Fig. 2b we show the corresponding interaction energy and associated lamellar phase deformation for two colloids of different radiuses.

Lamellar phases made of surfactants can have a much larger layer spacing (see Section II A 1), so that larger colloids can fit in. They also have weaker elastic constants, so that fluctuation effects are larger. We show in Figs. 2c and 2d the typical interaction energy and the corresponding lamellar phase deformation. The values correspond to $C_{12}E_5$ surfactants with colloids of diameter $\simeq 27\,\text{nm}$, as in the experiments of ref.17. The behaviours are similar to those of lipid membranes, but the energies are much smaller. Also the contribution of the Casimir interaction is no longer negligible.

3. Second virial coefficient

For membrane-binding colloids of diameter a dispersed in a lamellar phase, the second virial coefficient is given (in dimensionless form) by

$$B_2 = \frac{1}{2} \int d^2R \, dz \left(1 - e^{-F_{\text{bind}}(\mathbf{R}, p = z/d)} \right), \tag{30}$$

where the coordinate z is the vertical position of a colloid. Taking into account the discrete nature of the layers, we make the replacement $\int f(z)dz \to d\sum_p f_p$, thus obtaining

$$B_2 = \frac{\pi a^2 d}{2} \beta_2 \, , \tag{31}$$

with the normalized second virial coefficient

$$\beta_2 = 1 + \sum_{p=-\infty}^{\infty} \int_{\delta_{p,0}}^{\infty} dr \, 2r \left(1 - \frac{\exp\left(\frac{2\pi(a-w)^2}{1 + G_p(ar)^{-1}} \right)}{\sqrt{1 - G_p(ar)^2}} \right). \tag{32}$$

In the last equation, we have used eqns (24) and (25) and we have taken into account the excluded volume interaction between colloids in the same layer ($p = 0$). Note that with our normalization the pure hard core interaction corresponds to $\beta_2 = 1$.

The numerically calculated values of β_2 are shown in Fig. 3 as a function of the water thickness and colloid size. As we always have $\beta_2 < 1$, the interaction is always globally attractive. When $0 < \beta_2 < 1$, however, it doesn't prevail over the hard core, indicating a globally stable colloid dispersion.

B. Membrane-excluding colloids

Let us now consider colloids that interact with the membranes only through excluded volume forces, as the colloid on the left in Fig. 1. We take a first colloid of diameter a placed between layers $n = 0$ and $n = 1$ at the in-plane position $(x, y) = \mathbf{0}$, and a second one of diameter b placed between layers $n = p$ and $n = p + 1$ at the in-plane position $(x, y) = \mathbf{R}$. We model their presence in between the layers by imposing that the gaps between their neighboring membranes, on the axis normal to the undeformed membranes, cannot be smaller than their diameter. Such a constraint corresponds to the Hamiltonians of the infinite well type:

$$\mathcal{H}_a(z_a) = \begin{cases} 0 & \text{if } z_a \in [z_0(\mathbf{0}) + \frac{\delta+a}{2}, z_1(\mathbf{0}) - \frac{\delta+a}{2}], \\ +\infty & \text{otherwise,} \end{cases} \tag{33}$$

$$\mathcal{H}_b(z_b) = \begin{cases} 0 & \text{if } z_b \in [z_p(\mathbf{R}) + \frac{\delta+b}{2}, z_{p+1}(\mathbf{R}) - \frac{\delta+b}{2}], \\ +\infty & \text{otherwise,} \end{cases} \tag{34}$$

where z_a (resp. z_b) is the height of the particle of diameter a (resp. b) and $z_p(\mathbf{r}) = pd + h_p(\mathbf{r})$ is the height of the center of the membrane number p at the in-plane position $\mathbf{r}$.

The partition function, at fixed projected positions $\mathbf{0}$ and $\mathbf{R}$ of the colloids, is then given by

$$Z_{\text{ex}} = \int \left(\prod_{n=0}^{N-1} \mathcal{D}[h_n] \right) dz_a \, dz_b \, e^{-[\mathcal{H} + \mathcal{H}_a(z_a) + \mathcal{H}_b(z_b)]} \, . \tag{35}$$

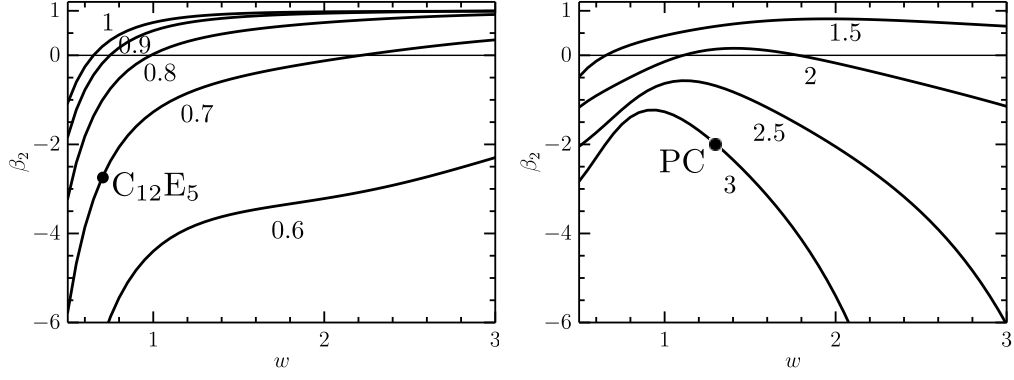Integrating the Boltzmann weights associated to the infinite

FIG. 3. Normalized second virial coefficient β_2 as a function of water thickness for the values of the ratio a/w indicated on the curves. The egg PC and $C_{12}E_5$ systems corresponding to Fig. 2 are indicated by the dots.
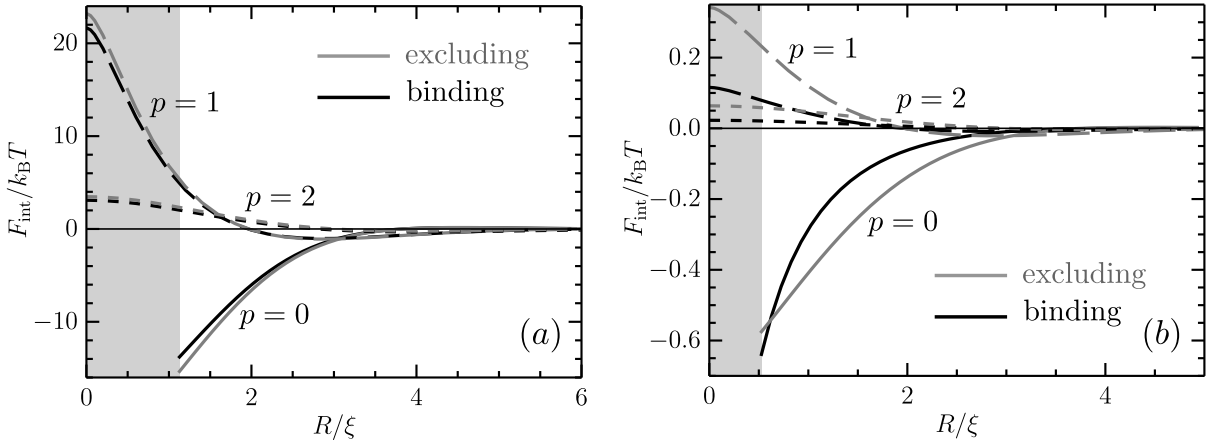

FIG. 4. Comparaison between the interaction energies of membrane-excluding colloids (gray lines) and of membrane-binding colloids (black lines, same curves as in Fig. 2a, c and d). Solid lines: colloids in the same layer ($p = 0$), long-dashed lines: colloids one layer appart ($p = 1$), dashed-line: colloids two layers appart ($p = 2$). (a) Lamellar phase with the parameters of egg PC and colloids of diameter $a = b = 3w$. (b) Lamellar phase with the parameters of $C_{12}E_5$ and colloids of diameter $a = b = 0.7w$.

wells gives simply

$$\int dz_a\, e^{-\mathcal{H}_a(z_a)} = (H_0(\mathbf{0}) - a)\,\Theta\,(H_0(\mathbf{0}) - a)\,, \qquad (36)$$

$$\int dz_b\, e^{-\mathcal{H}_b(z_b)} = (H_p(\mathbf{R}) - b)\,\Theta\,(H_p(\mathbf{R}) - b)\,, \qquad (37)$$

where $H_0(\mathbf{0}) - a$ (resp. $H_p(\mathbf{R}) - b$) is the gap available to the first (resp. second) colloid and the Heaviside functions Θ are such that the integrals vanish when the gaps are smaller than the colloids diameters. Using the relation $\Theta(x - a) = \int_a^\infty dg\,\delta(x - g)$, we can map the problem onto that of binding colloids, yielding

$$Z_{\mathrm{ex}}(R, p) = \int_a^\infty dg \int_b^\infty dg'\,(g - a)(g' - b)\,Z_{\mathrm{bind}}(g, g')\,, \qquad (38)$$

where $Z_{\mathrm{bind}}(g, g')$ is the partition function for binding colloids of diameters g and g', obtained by replacing a and b

by g and g' in eqn 22. This expression can be understood if one thinks of integrating first over the gaps $g \in [a, \infty]$ and $g' \in [b, \infty]$ of the layers surrounding the colloids, then over the other degrees of freedom at fixed gaps: the integration of the membrane degrees of freedom at fixed gaps gives the partition function (22) for membrane-binding colloids, while the integration over the particle positions gives the entropic contributions $g - a$ and $g' - b$.

1. Interaction free energy and average deformation

The interaction free energy for two membrane-excluding colloids is therefore given by

$$F_{\mathrm{ex}}(R, p) = -\ln \frac{Z_{\mathrm{ex}}(R, p)}{Z_{\mathrm{ex}}(+\infty, p)}\,, \qquad (39)$$

which can be easily calculated numerically by a double integration. Note that it is no longer possible here to extract

separately an elastic contribution and a Casimir one.

The average deformation of the layers can be calculated by adding to the partition function (35) an external field J as in eqns (16)–(17). From the relation $\langle h_{-Q,-\boldsymbol{q}} \rangle_{\mathrm{ex}} = (1/Z_{\mathrm{ex}})\partial Z_{\mathrm{ex}}/\partial J_{Q,\boldsymbol{q}}|_{J=0}$, using $\partial Z_{\mathrm{bind}}(g,g')/\partial J_{Q,\boldsymbol{q}}|_{J=0} = \langle h_{-Q,-\boldsymbol{q}} \rangle_{\mathrm{bind}} \times Z_{\mathrm{bind}}(g,g')$ yields in direct space:

$$\langle h_n(\boldsymbol{r}) \rangle_{\mathrm{ex}} = \frac{1}{Z_{\mathrm{ex}}} \int_a^\infty dg \int_b^\infty dg' \, (g-a)(g'-b)$$
$$\times \, \langle h_n(\boldsymbol{r}) \rangle_{\mathrm{bind}} \, Z_{\mathrm{bind}}(g,g'), \qquad (40)$$

with $\langle h_n(\boldsymbol{r}) \rangle_{\mathrm{bind}}$ the average layer deformation at projected position $\boldsymbol{r}$ for two colloids of diameters g and g'. This expression can also be understood intuitively, since $\langle h_n(\boldsymbol{r}) \rangle_{\mathrm{bind}} Z_{\mathrm{bind}}$ is the integral over all the microstates corresponding to fixed gaps g and g' of $h_n(\boldsymbol{r})$ multiplied by $\exp(-\mathcal{H})$.

Since for one isolated binding colloid of radius g we have $\langle H_0 \rangle_{\mathrm{bind}} = g$ and $Z_{\mathrm{bind}} = C \exp[-\pi(g-w)^2]$ (see eqn (22)), the average gap $\langle H_0^{(1)} \rangle$ set by one hard-core colloid of radius a is given by

$$\langle H_0^{(1)} \rangle_{\mathrm{ex}} = \frac{\int_a^\infty (g-a)g \, e^{-\pi(g-w)^2}}{\int_a^\infty (g-a) \, e^{-\pi(g-w)^2}}$$
$$= w + \left(2\pi(w-a) + \frac{2e^{-\pi(a-w)^2}}{\mathrm{erfc}[\sqrt{\pi}(a-w)]} \right)^{-1}. \qquad (41)$$

2. Typical results

In Fig. 4 we compare the interaction energies between membrane-excluding and membrane-binding colloids for egg PC lipids with colloids of diameters $\simeq 3\,\mathrm{nm}$ and for $C_{12}E_5$ surfactants with colloids of diameter $\simeq 27\,\mathrm{nm}$, as in Fig. 2.

In the case of egg PC lipids, the colloid diameters are much larger than the average water thickness. Then, the configurations that are effectively sampled by the fluctuations do not significantly depend on whether the colloids stick to the layers or not, as spreading the layers further away from the colloids costs a large energy. This is why, the interaction energies for the membrane-excluding and membrane-binding cases are very close (see Fig. 4a).

Conversely, in the case of $C_{12}E_5$ surfactants, the colloid diameters are slightly smaller than the average water thickness. Therefore, the interaction between membrane-excluding colloids is of pure fluctuation (Casimir) origin: in the absence of fluctuations, the colloids sit anywhere in between the layers without producing any deformation, whatever their distance. As seen in Fig. 4b, in this case, the interaction energies for the membrane-excluding and membrane-binding cases differ significantly, even though the overall behavior is similar. Due to the various contributions to the free energies (elastic deformations, entropy associated to the fluctuations of the membranes and of the colloids) and their differences in the two situations, it is difficult to get a qualititative understanding of the interaction energy variations between the two situations.

IV. MONTE CARLO SIMULATIONS

To investigate the equilibrium statistical behavior of the interacting colloids, we use a Monte Carlo simulation with a Metropolis algorithm. We simulate only the behavior of the colloidal particles, subjected to the membrane-mediated interaction that we have previously computed. Precisely, we model the colloid-lamellar phase system as a finite number M of stacks of identical colloids orthogonal to z-direction, each one consisting of the same finite number N of particles confined in a disk of radius R_d. We suppose that the particles cannot change stack. To simplify, we consider only pairwise interactions (i.e., we neglect multibody effects) and we take into account only the contributions coming from particles in the same layer and one layer apart. Indeed, as we saw in Section III, the interaction decreases rapidly with the layer separation. Moreover, since the interactions are short-ranged, we do not impose periodic boundary conditions within each layer, but we do use periodic boundary conditions in the z-direction, such that a small number ($\simeq 7$) of layers is enough for simulating an infinite system.

We start the simulation by placing the same number N of particles in each one of the M layers according to a random uniform distribution respecting a given hard-core minimum distance a_0. We then pick at random one particle and we move it randomly inside a circle of radius ϵ. We compute the associated variation of the interaction energy and we accept the movement according to the Metropolis rule, taking into account the hard-core constraint. The radius ϵ is adjusted in order to have an acceptance ratio of $\simeq 50\%$. The interaction energy between two colloids is computed according to eqn (23) [resp. (39)] for the membrane-binding (resp. membrane-excluding) case, where the correlation functions $G_0(R)$ and $G_1(R)$ [see eqn (11)] can be expressed analytically in terms of modified Bessel functions, as shown in the Appendix.

After equilibration, we characterize the statistical order of the colloids by means of the structure factor [34, 35]:

$$S(\boldsymbol{q}, Q) = \frac{1}{MN} \left\langle \left| \sum_{j,p} \exp\left[i \left(\boldsymbol{q} \cdot \boldsymbol{R}_{jp} + pQd \right) \right] \right|^2 \right\rangle,$$
$$= S_0(\boldsymbol{q}) + 2 \sum_{n=1}^\infty S_n(\boldsymbol{q}) \cos(nQd), \qquad (42)$$

where $\boldsymbol{R}_{jp}$ is the position of the j-th particle of the p-th layer and $\boldsymbol{q}$ (resp. Q) is the component of the wavevector parallel (resp. perpendicular) to the lipid layers. The structure factor is proportional to the Fourier transform of the two-particle correlation function. Note that in eqn (42) we neglect the fluctuations of the colloids in the z-direction. The partial structure factors $S_n(\boldsymbol{q})$ describe the correlations between particles n layers apart.

For a liquid-like order, the structure factors do not depend on the orientation of the $\boldsymbol{q}$ vector and thus coincide with their
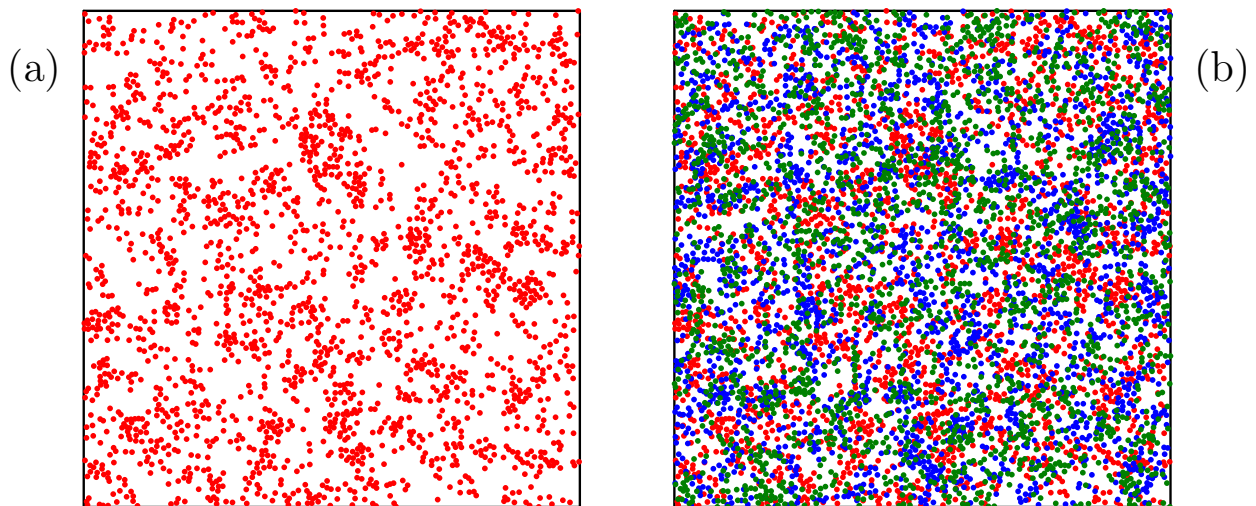
FIG. 5. Typical snapshot of a Monte Carlo simulation of the membrane-excluding colloids (after equilibration) for the parameters of $C_{12}E_5$ (see Section II A 2) for particles of diameter $a = 27\,\mathrm{nm}$ and hard-core distance between colloids of $34\,\mathrm{nm}$. The colloid volume fraction is 2%. The colloids in one layer are represented as red disks. The blue and green disks represent the colloids in the two adjacent layers. The diameter of the disks corresponds to the hard-core distance. (a) Colloids in one layer. (b) Red disks: same layer of colloids as in (a); blue and green disks: colloids in the adjacent two layers for the same snapshot.

average with respect to the orientation of $\boldsymbol{q}$:

$$S_n(q) = \frac{1}{MN} \left\langle \sum_{i,j=0}^{N-1} \sum_{p=0}^{M-1} \mathrm{J}_0\left(q\left|\boldsymbol{R}_{ip} - \boldsymbol{R}_{j(p+n)}\right|\right) \right\rangle ,$$

(43)

where q is the modulus of $\boldsymbol{q}$ and because of the periodic boundary conditions in the direction perpendicular to the layers, layers p and $p + M$ coincide.

In Fig. 5 we show a typical Monte Carlo snapshot of three successive layers (blue, red, and green disks) for membrane-excluding colloids of diameter $27\,\mathrm{nm}$ embedded in a lamellar phase with the parameters of $C_{12}E_5$. The corresponding interaction energy is displayed in Figs. 2c and 2d. To the membrane-mediated energy we added a hard core interaction with an effective core diameter of $34\,\mathrm{nm}$, as measured in aqueous solution. (see Section V). Clearly, the colloids in each layer tend to aggregate in large clusters. Moreover, the clusters are statistically anticorrelated between adjacent layers: clusters in a layer tends to face voids in the adjacent layers. This organization originates from the attractive (resp. repulsive) character of the interaction between two colloids sitting in the same layer (resp. one layer apart), as shown in Figs. 2c and 2d.

For the same parameters, the membrane-binding colloids tend also to form clusters, although they are less marked (see Fig. 6). To assess them, we show in the inset of Fig. 6 the intra-layer structure factor S_0 (solid line). For comparison, we also show (dashed line) the structure factor S_0 obtained by switching off the interactions, thus taking into account only the hard core contribution. The first maximum at $q \simeq 0.16\,\mathrm{nm}^{-1}$ corresponds to the hard core diameter of the particles. At smaller wavevectors, the structure factor in presence of interaction shows a rise for $q \to 0$ that is absent in the case of hard core only interaction (dashed line). This can

be understood as due to the form factor of random fluctuating clusters with a distribution of sizes down to $2\pi/q_{\min}$, where $q_{\min}$ is the position of the minimum of S_0 close to $q = 0$. Indeed, $q_{\min}$ gives an upper estimate of the size of the peak at $q = 0$. In the snapshot we have indicated this size by surrounding small clusters in two adjacent layers. This is compatible with the fact that, as shown in Fig. 4b, the interaction energy for membrane-binding colloids has the same overall shape, but lower amplitude in comparison with membrane-excluding ones. Increasing the particle concentration results in a similar cluster structure in a denser system.

In the literature, the structure factors of pairwise interacting particles are often calculated in the framework of the Ornstein-Zernicke relation with the approximate Percus-Yevick closure, using the numerical method introduced by Lado [36, 37]. Mapping our multilayer problem to a multi-component fluid, as done in ref. 35, we have computed the equatorial structure factor $S(q) = S_0(q) + 2S_1(q)$ that can be measured by small-angle X-ray scattering with a scattering vector contained in the plane of the layers (see Section V). At small concentrations, we find that the Percus-Yevick approximation is reasonably good (see Fig. 7). However, at higher concentrations for our system the Lado algorithm does not converge in general.

V. SAXS

The small-angle X-ray scattering (SAXS) data was acquired as described in ref. 17. Briefly, we performed scattering experiments on oriented lamellar stacks of $C_{12}E_5$ surfactants, with silica particles of nominal diameter of $27\,\mathrm{nm}$, at normal incidence (the beam is parallel to the smectic director). We recorded the two-dimensional intensity $I(q = |\mathbf{q}|)$,
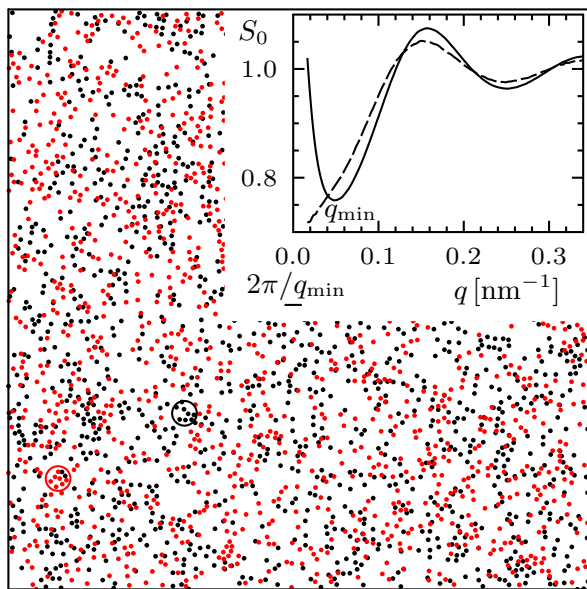
FIG. 6. Typical snapshot of a Monte Carlo simulation of the membrane-binding colloids (after equilibration). The black disks are in one layer and the red disks in an adjacent one. The diameter of the disks corresponds to the hard core of the colloids. Inset: structure factor $S_0(q)$ inside the layers in the presence of the interparticle interaction (continuous line) and only with hard core repulsion (dashed line). The position $q_{\min}$ of the minimum of $S_0(q)$ gives an upper estimate of the width of the peak at $q = 0$. The corresponding length $2\pi/q_{\min}$ is materialized by the bar and by the diameter of the black and red circles surrounding small clusters in two adjacent layers. The parameters of the Monte Carlo simulation correspond to the values given in Section V for a colloid volume fraction of 2%.

with $\mathbf{q} = (q_x, q_y)$ the scattering vector in the plane of the layers and $Q = 0$ the scattering vector othogonal to the layers. The structure factors of the various samples (see Fig. 8) were obtained as $S(q) = S(q, Q = 0) = I(q)/|F(q)|^2$, where $|F(q)|^2$ is the form factor of the particles, measured in aqueous suspension. Note that eqn (42) is valid only for the perfect case where the particles do not fluctuate in the z-direction. The thermal fluctuations and the frozen-in defects lead to a smearing of the diffraction pattern an high Q values, that we describe phenomenologically by a Lorentzian factor [35]

$$S(\mathbf{q}, Q) = S_0(\mathbf{q}, Q) + 2\frac{\cos(Qd)}{1 + (Q\sigma)^2}S_1(\mathbf{q}), \qquad (44)$$

where the disorder parameter σ has units of length.

A. Membrane-binding predictions

We compare the measured structure factors with our Monte Carlo simulations, described in Section IV. For the latter, we adjusted the radius R_d of the simulation box and the number of layers in order to have convergence for the correlation functions. Clearly, using only the hard-core repulsion (dashed blue line in Fig. 8a), with an effective core diameter of 34 nm
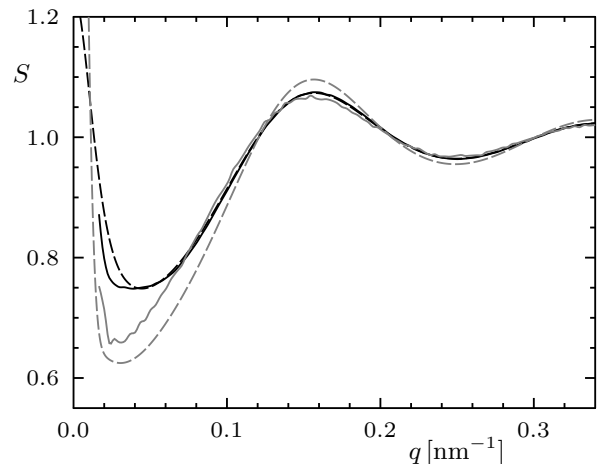

FIG. 7. Comparison of the equatorial structure factor $S(q) = S_0(q) + 2S_1(q)$ computed with a Monte Carlo simulation (full lines) and the Percus-Yevick approximation (dashed lines). The black (resp. gray) curves correspond to the membrane-binding (resp. membrane-excluding) case. The parameters of the Monte Carlo simulation correspond to the values given in Section V for a colloid volume fraction $\phi = 2\%$.

describing the interaction measured in aqueous solution (the core is larger than the nominal diameter due to the electrostatic repulsion), does not yield a good description of the experimental data on the left of the structure peak ($q < 0.15\,\mathrm{nm}^{-1}$).

Including the membrane-binding colloid interaction, with the elastic parameters of $\mathrm{C}_{12}\mathrm{E}_5$ surfactants given in Table I, captures quantitatively, with no adjustable parameters, the experimental points down to the small-angle increase ($q > 0.05\,\mathrm{nm}^{-1}$). The latter ($q < 0.05\,\mathrm{nm}^{-1}$) is described qualitatively by the complete model, while it is obviously absent in a hard-core system.

B. Membrane-excluding predictions

The membrane-excluding model (Fig. 8b) also predicts a small-angle increase, which is however less important than for the binding case; overall, this model agrees less well with the experimental data.

VI. CONCLUSION

We treated in detail the interaction between hard spherical inclusions in lyotropic smectics, for the limiting cases of membrane-excluding and membrane-binding particles. In both cases, the interaction range is of the order of the elastic correlation length $\xi = (\kappa/B)^{1/4} = \sqrt{\lambda d}$ defined in Section II. For membrane-binding colloids of identical diameters a, the interaction energy (23) at contact, in the limit $a \ll \xi$, is approximatively given, in dimensionful form, by

$$F_{\mathrm{bind}}^{\mathrm{contact}} \simeq \frac{k_{\mathrm{B}}T}{2}\log C + \frac{\pi}{4}(C - 4)\sqrt{B\kappa}(a - w)^2, \quad (45)$$
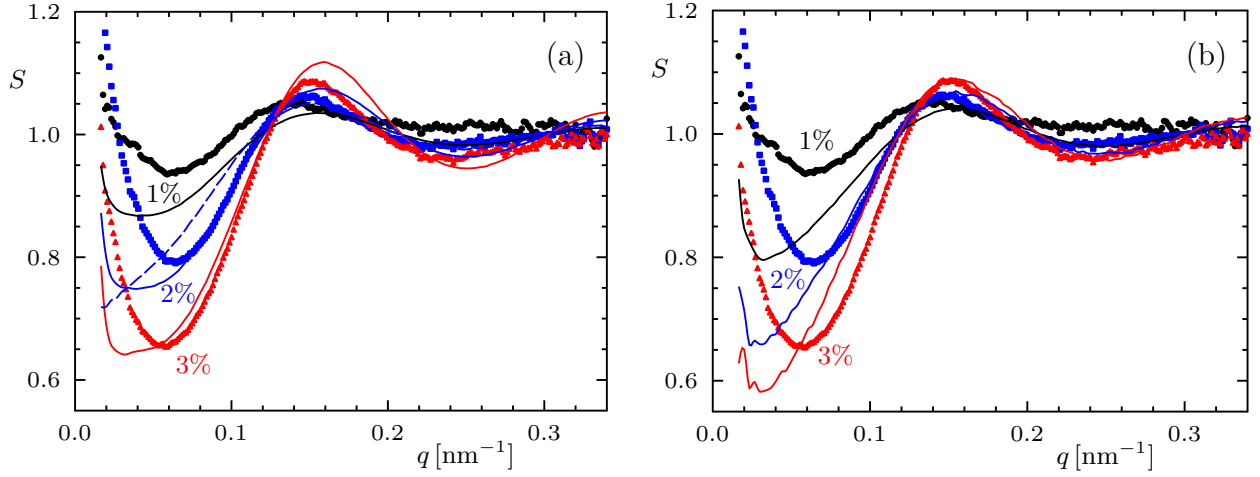
FIG. 8. Experimental in-plane structure factors for silica nanoparticles confined in lamellar phases at three different volume concentrations ϕ [17] (black circles: $\phi = 1\%$; blue squares: $\phi = 2\%$; red triangles: $\phi = 3\%$) and Monte Carlo predictions according to our model (solid lines). (a) Membrane-binding inclusions. (b) Membrane-excluding inclusions. Black solid lines: $\phi = 1\%$; blue solid lines: $\phi = 2\%$; red solid lines: $\phi = 3\%$. The dashed blue line in (a) is the simulated structure factor for $\phi = 2\%$ with only hard-core interactions. To obtain convergence, in the membrane-binding [resp. membrane-excluding] case, the Monte Carlo averages are performed on 10^7 (resp. 3×10^8) steps after equilibration on a system consisting of 7 layers having a reduced radius $R = 20$ (resp. $R = 160$).

where

$$C = \left(\frac{a}{\xi}\right)^2 \left[\ln\left(\frac{\xi}{a}\right) + \frac{3}{4} + \log 2 - \gamma\right], \qquad (46)$$

with $\gamma \simeq 0.577$ the Euler constant. This contact energy varies from tens of k_BT for lipid systems to fractions of k_BT in dilute phases of single-chain surfactants.

For systems of the latter type we compared our predictions to experimental structure factors measured at three concentrations of silica nanoparticles in a dilute lamellar phase of nonionic surfactant. We obtain semi-quantitative agreement with no adjustable parameters. Remarkably, this agreement is significantly better for the membrane-binding model than for the membrane-excluding one, consistent with strong adsorption of these surfactants onto silica surfaces, a result widely accepted in the literature (see, e.g., the discussion in ref. 38.)

The presence of the particles acts as a constraint on the membrane fluctuations, leading to an attractive "Casimir-like" component of the interaction, which is quite significant (or even dominant) for the surfactant systems discussed above.

For strongly attractive systems (with a negative second virial coefficient), the liquid of particles is unstable with respect to aggregation. The peculiar nature of the interaction (overall attractive in the plane of the layers and repulsive across the layers) leads to the formation of flat and size-limited aggregates. As a concrete application, one could consider dispersing the particles into a host lamellar phase with suitably chosen parameters so that they remain well separated, and then inducing their aggregation by an external stimulus (temperature change, controlled drying, etc) that increases the interparticle attraction. The resulting assemblies could then be stabilized by various strategies [39].

APPENDIX

Performing the integral in ϕ in eqn. 11 by means of the residue theorem, the correlation function inside one layer can be written as

$$G_0(r) = \int_0^\infty \left(q - \frac{q^3}{\sqrt{q^4 + 4}}\right) J_0(qr) \, dq. \qquad (47)$$

We use the integral [40]

$$\int_0^\infty q^{1-\nu} J_\nu(qr) \, dq = \frac{r^{\nu-2}}{2^{\nu-1}\Gamma(\nu)} \qquad (48)$$

for $\mathrm{Re}(\nu) > 1/2$, where $\Gamma(\nu)$ is the gamma function, and, for $\mathrm{Re}(\nu) > 1/6$, the integral [40]

$$\int_0^\infty \frac{q^{\nu+3}}{(q^4+4)^{\nu+1/2}} J_\nu(qr) \, dq = \frac{r^\nu \sqrt{\pi}}{2^{3\nu-1}\Gamma(\nu+\frac{1}{2})} J_{\nu-1}(r) K_{\nu-1}(r). \qquad (49)$$

Then, taking the difference between eqn (48) and (49), by analytical continuation we get, in the limit $\nu \to 0$,

$$G_0(r) = 2J_1(r) K_1(r). \qquad (50)$$

Similarly, the correlation function (11) one layer apart can be expressed as

$$G_1(r) = \int_0^\infty \left(\frac{q^5}{2} - \frac{q^3}{\sqrt{q^4+4}} - \frac{q^7}{2\sqrt{q^4+4}} \right) \mathrm{J}_0(qr)\, dq\,.$$

(51)

Proceeding as before, it is then easily found that

$$G_1(r) = \left[\left(\frac{32}{r^3} - \frac{4}{r} \right) \mathrm{J}_1(r) - \frac{16}{r^2} \mathrm{J}_0(r) \right] \mathrm{K}_0(r)$$
$$+ \left[\left(\frac{64}{r^4} - 2 \right) \mathrm{J}_1(r) - \left(\frac{32}{r^3} + \frac{4}{r} \right) \mathrm{J}_0(r) \right] \mathrm{K}_1(r)\,.$$

(52)

[1] H. K. Bisoyi and S. Kumar, *Chem. Soc. Rev.*, 2011, **40**, 306–319.

[2] R. Pratibha, K. Park, I. I. Smalyukh and W. Park, *Optics express*, 2009, **17**, 19459–19469.

[3] Q. Liu, Y. Yuan and I. I. Smalyukh, *Nano Letters*, 2014, **14**, 4071–4077.

[4] M. Wojcik, W. Lewandowski, J. Matraszek, J. Mieczkowski, J. Borysiuk, D. Pociecha and E. Gorecka, *Angewandte Chemie (International Ed. in English)*, 2009, **48**, 5167–5169.

[5] D. Coursault, J. Grand, B. Zappone, H. Ayeb, G. Lévi, N. Félidj and E. Lacaze, *Advanced Materials*, 2012, **24**, 1461–1465.

[6] W. Lewandowski, D. Constantin, K. Walicka, D. Pociecha, J. Mieczkowski and E. Górecka, *Chemical Communications*, 2013, **49**, 7845–7847.

[7] Q. Liu, Y. Cui, D. Gardner, X. Li, S. He and I. I. Smalyukh, *Nano Letters*, 2010, **10**, 1347–1353.

[8] E. Venugopal, S. K. Bhat, J. J. Vallooran and R. Mezzenga, *Langmuir*, 2011, **27**, 9792–9800.

[9] W. Wang, S. Efrima and O. Regev, *The Journal of Physical Chemistry B*, 1999, **103**, 5613–5621.

[10] M. A. Firestone, D. E. Williams, S. Seifert and R. Csencsits, *Nano Letters*, 2001, **1**, 129–135.

[11] D. Constantin and P. Davidson, *ChemPhysChem*, 2014, **15**, 1270–1282.

[12] E. Henry, A. Dif, M. Schmutz, L. Legoff, F. Amblard, V. Marchi-Artzner and F. Artzner, *Nano Letters*, 2011, **11**, 5443–5448.

[13] J. Yamamoto and H. Tanaka, *Nature Materials*, 2005, **4**, 75–80.

[14] R. Hołyst, *Physical Review A*, 1991, **44**, 3692–3709.

[15] N. Lei, C. R. Safinya and R. F. Bruinsma, *J Phys II France*, 1995, **5**, 1155–1163.

[16] S. A. Safran, *Statistical thermodynamics of surfaces, interfaces, and membranes*, Addison-Wesley, Reading, Massachusetts, 1994.

[17] K. Béneut, D. Constantin, P. Davidson, A. Dessombz and C. Chanéac, *Langmuir*, 2008, **24**, 8205.

[18] W. Helfrich, *Z. NaturForsch.*, 1978, **A 83**, 305.

[19] D. Roux and C. R. Safinya, *Journal de Physique*, 1988, **49**, 307–318.

[20] Y. S. Jho, M. W. Kim, S. A. Safran and P. A. Pincus, *The European Physical Journal E*, 2010, **31**, 207–214.

[21] W. Helfrich, *Z. NaturForsch.*, 1973, **C 28**, 693.

[22] P.-G. de Gennes, *J. Phys. (Paris), Colloq.*, 1969, **30**, C4–65.

[23] C. A., *C. R. Séances Acad. Sci., Ser. B*, 1972, **174**, 891.

[24] H. I. Petrache, N. Gouliaev, S. Tristram-Nagle, R. Zhang, R. M. Suter and J. F. Nagle, *Physical Review E*, 1998, **57**, 7014–7024.

[25] E. Freyssingeas, F. Nallet and D. Roux, *Langmuir*, 1996, **12**, 6028.

[26] P. M. Chaikin and T. C. Lubensky, *Principles of condensed matter physics*, Cambridge University Press, Cambridge, US, 1995.

[27] P. Sens and M.S. Turner, *J. Phys. II France*, 1997, **7**, 1855–1870.

[28] M. S. Turner and P. Sens, *Phys. Rev. E*, 1997, **55**, R1275–R1278.

[29] M. S. Turner and P. Sens, *Phys. Rev. E*, 1998, **57**, 823–828.

[30] P. Sens and M. Turner, *The European Physical Journal E*, 2001, **4**, 115–120.

[31] P.-G. de Gennes and J. Prost, *The Physics of Liquid Crystals*, Oxford Science Publications, Oxford, 1993.

[32] O. M. Tovkach, J.-i. Fukuda and B. I. Lev, *Phys. Rev. E*, 2013, **88**, 052502.

[33] C. D. Santangelo and R. D. Kamien, *Phys. Rev. Lett.*, 2003, **91**, 045506.

[34] L. Yang, T. Weiss, T. Harroun, W. Heller and H. Huang, *Biophys. J.*, 1999, **77**, 2648–2656.

[35] D. Constantin, *The Journal of Chemical Physics*, 2010, **133**, 144901.

[36] F. Lado, *J. Chem. Phys.*, 1967, **47**, 4828.

[37] F. Lado, *J. Chem. Phys.*, 1968, **49**, 3092.

[38] K. P. Sharma, V. K. Aswal and G. Kumaraswamy, *The Journal of Physical Chemistry B*, 2010, **114**, 10986–10994.

[39] M. A. Boles, M. Engel and Talapin, *Chemical Reviews*, 2016, **116**, 11220–11289.

[40] G. Watson, *A Treatise on the Theory of Bessel Functions (2nd ed.)*, Cambridge University Press, Cambridge, US, 1966, p. 435.